Metrology of IXO Mirror Segments

Kai-Wing Chan*[a,d], Melinda Hong[b], Timo Saha[c], William Zhang[d]

[a]Center for Research and Exploration in Space Science and Technology & Center for Space Science and Technology, University of Maryland, Baltimore County, Baltimore MD 21250, USA
[b]SGT, Inc., 7701 Greenbelt Road, Greenbelt, MD 20770, USA
[c]Optics Branch, NASA/Goddard Space Flight Center, Greenbelt, MD 20771, USA
[d]X-Ray Astrophysics Laboratory, NASA/Goddard Space Flight Center, Greenbelt, MD 20771, USA

ABSTRACT

For future x-ray astrophysics mission that demands optics with large throughput and excellent angular resolution, many telescope concepts build around assembling thin mirror segments in a Wolter I geometry, such as that originally proposed for the International X-ray Observatory. The arc-second resolution requirement posts unique challenges not just for fabrication, mounting but also for metrology of these mirror segments. In this paper, we shall discuss the metrology of these segments using normal incidence metrological method with interferometers and null lenses. We present results of the calibration of the metrology systems we are currently using, discuss their accuracy and address the precision in measuring near-cylindrical mirror segments and the stability of the measurements.

Keywords: X-ray optics; Lightweight mirror; Metrology; Normal incidence metrology

1. INTRODUCTION

High throughput, lightweight x-ray optics with arc-second angular resolution, is expected to be key technological development capable of opening up discovery space in astrophysics. A mission with optics similar to that originally planned for the International X-ray Observatory---despite its termination due to Astrophysics and Planetary decadal rankings and NASA´s constrained resources projected---will enable significant discoveries in astrophysics with high-resolution imagining spectroscopy in the x-ray band.

A basic approach to realize a lightweight, compact, telescope with substantial effective area is to build a segmented telescope that is assembled from individual modules consisting of densely packed mirror shells in a Wolter type I geometry. The challenge of such optics lies in producing modular optics from aligning and integrating thin mirror segments with excellent angular resolution. As these mirror substrates are very thin, they are also not very stiff, making the building of such optics opto-mechanically challenging. Presently, our team of researchers at NASA's Goddard Space Flight Center are developing technology to build a module with segmented reflectors capable of reaching arc-second resolution, using glass mirror segments as thin as 0.4 mm and with a size of about 200 mm. Within these broad parameters, the critical challenges are to produce individual mirror substrates with arc-second resolution before mounting, to be able to mount these mirrors into a housing structure without introducing arc-second distortion, and to be able to measure the performance with sub-arc-second accuracy. In this paper, we will discuss our effort in measuring the performance of these mirrors.

Currently, glass mirrors (Schott D264) are thermally slumped on precision mandrels to attain its perfect form for x-ray focusing. The forming process aims for the glass segment to take up precise low order figure of the mandrel. High-frequency surface properties, which are inherent in the glass and is acceptable from the original smooth glass substrate, is preserved in the thermoforming. The mirror is subsequently mounted onto a strongback ("temporary-mount") enabling it to be measured, aligned and finally integrated ("permanent mount"). Measurements are made after the mirrors are initially formed, after they are temporary-mounted, and after they are permanently mounted.

1.1 Metrology of mirror segments

For a given mirror, typically of size 200 mm by 30°, we measure its low order figure error, mid-frequency error and micro-roughness in order to assess its overall performance. Micro-roughness can be measured with a surface profiler or x-ray diffractometer. We routinely use a profiler (Zygo NewView), which is capable of 0.1 nm resolution in mm scale down to tens of μm, to measure surface micro-roughness optically. However, we will not be discussing micro-roughness further here since it is not a critical parameter that needs further improvement, and it is also an inherent property of the glass that is preserved in the processing of the mirror. Mid-frequency errors, in the spatial scale of $\approx 2 - 20$ mm, are measured by surface metrology described below. Like micro-roughness, error at this scale is preserved in the slumping process and we will not address it further in this paper. The significance and reliability of the mid-frequency errors will be addressed elsewhere.

In this paper, we will concentrate on low order figure distortion that arise essentially from mounting the mirror, including the metrology mount. To that end, we employ normal incidence metrology by using Fizeau interferometer coupled with refractive null lens to generate cylindrical wavefront for the measurement[1,2]. The advantages of this metrological method are: (1) It is relatively fast. Measurement time after the mirror is set up takes only seconds, compared with much longer time with scanning methods[3,4,5,6]. Long measuring time is not only inefficient but the measurement is susceptible to mechanical, thermal or other drifts. (2) The whole surface is measured simultaneously without any need to stitch data as in, for example, using interferometer without the null lens to measure azimuth-by-azimuth[7]. Error propagation from data stitching is therefore avoided. (3) The system can be calibrated with simple good flat reference, without the need to develop sophisticated aspheric optics or other absolute references[8]. An alterative to using a null lens may be the use of a computer-generated hologram[9].

With his method, not only the full mirror surface can be measured with high precision in a relatively short time, the measurement covers a large span of scales, from 200 mm down to mm spatial scale, in both azimuthal and axial directions. For the measurement of mirrors at hand, we will, however, concentrate on the measurements of axial figure errors as azimuthal errors are usually relatively benign due to small grazing angles. We will focus especially on radius and radius variation, cone angle and its variation, sag and sag variation. We will address third and higher order errors when it is important, for example, when a mirror is constrained at it sides by 3 or more points.

We will discuss the normal incidence surface metrology with Fizeau interferometers in Section 2.1. The measurement gives axial figure at all azimuths. All low order axial figure errors can, in principle, be derived from the measurement. Cone angle error, however, is not reliably measured since the measurement is sensitive to the orientation of the mirror that is not precisely controlled. For example, yawing of the mirror (i.e., rotation about a radius vector roughly normal to the surface of the mirror) produces additional error of cone angle which depends linearly on azimuth. (For a yaw angle of β, the correction is $4\beta \sin(\phi)$, where ϕ is the azimuthal angle measured from the middle azimuth. For example, for a mirror with an angular span of $\Omega = 30°$, maximum $4 \sin(\phi) = 1.0$ and cone angle error is as large as the yaw angle β. Sag error due to yaw, however, is quadratic in β and is generally small. In fact, the sag dependence due to yaw is approximately $2R\,(\beta \sin(\phi)/2)^2$ which is typically negligible.) To measure the cone angle, we rely on grazing incidence sub-aperture Hartmann test. We do not, at this point, measure absolute radius of a mirror. A cylindrical CMM measurement was attempted previously but the precision is limited by factors such as mirror vibration, alignment, and also mechanical and thermal drifts. We shall take up the radius measurement again after the sag and cone angle measurements are more precisely controlled. The overall performance including all error components, however, can be measured with direct x-ray test.

Precision of surface measurements using Fizeau interferometer system with cylindrical null lenses will be addressed in section 3. In terms of the absolute accuracy, the biggest error is in the null lenses themselves. We will address the issue of calibration in section 3.1. Metrology of the thin mirrors naturally dependence on the set up of a metrology mount. We have been using two mounts for metrology: a "cantor-tree" (CT) mount and a kinematic mount with 3 balls attached to the mirror (KB3). Repeatability of the metrology mounts, as well as the temporary mount, will be addressed in section 3.2. In section 3.3, we will discuss the measurement instability due to thermal drift.

2. FULL SURFACE METROLOGY AND CALIBRATION

Two sets of cylindrical null lenses were custom designed and fabricated for normal incidence metrology with interferometers[2]. Two interferometers manufactured by 4D Tehnologies, FizCam 1500 and FizCam 2000, are used for this purpose. The interferometers were chosen for its fast response with dynamic interferometry over general phase-shifting interferometers so that the mirrors can be sampled much faster (15 frame/s) to minimize effects due to mirror vibration. The interferometers are equipped with λ/20 transmission flats and the accuracy is therefore limited by the accuracy of the null lenses. Typically, the measurement returns a full surface map from which axial and azimuthal parameters can be derived. As mentioned above, the absolute radius and cone angle are not measured, as they depend on the placement and orientation of the mirror relative to the cylindrical null. It is conceivable that, if some reference is made with respect to the null lenses, these quantities can be measured. We will focus on the axial sag which plays a significant role in the performance of the x-ray mirrors.

2.1 Calibrations of FizCam 1500 and FizCam 2000.

To establish the reliability of the surface measurement, the null lenses were calibrated. The two FizCam setups are listed in the Table 1. Besides pairing up with null lens of different sizes, the two interferometers have different characteristics and measurement capabilities. The FizCam 2000 has a laser source with very short coherent length specified at 0.3 mm. It is therefore capable of measuring transparent mirrors with small thickness, such as our mirror of 0.4 mm, and yet not confused by fringes from backside reflection of the transparent part. However, this instrument does not work well for highly reflective mirrors due to large mismatch of intensities of the reference and return beams. The FizCam 1500, on the other hand, has a long coherent length and is designed for reflective surface. Surface with low reflectivity (lower than ~ 40%) is difficult with this instrument.

Table 1. Interferometers used for normal incidence surface metrology and their cylindrical null lenses.

	FizCam 1500	**FizCam 2000**
Transmission Flat		
Size	10 inch	12 inch
Quality	λ/20	λ/20
Null Lens		
Number of elements	4	2
Angular Span	60°	36°
Height	217 mm	217 mm

Calibration of FizCam 1500 with 60-degree Cylindrical Null. The 60° null lens was calibrated before with the FizCam 1500 using a flat mirror at different azimuth angles. Measurement were generally made with 5° increments over a span of about 56°. The resulting distribution of sag, over 200 mm, can be represented by the following form: $S(\phi) = A + B(\phi - \phi_0)^2 + C_1 \exp(-(\phi-\phi_1)^2/w_1) + C_1 \exp(-(\phi-\phi_2)^2/w_2)$.

The sag is dominated by the constant term, A, which is about 3 μm. The quadratic terms has a peak-to-peak variation over the 60° degree range of about 0.3 μm. The exponential terms fit the gentle profile with $C_{1,2} \approx 0.2$ μm and $w_{1,2} \approx (6 \text{ degree})^2$. The coordinate is defined such that the plane of symmetry of the null lens is at $\phi = 0$, with an extent by design of 30°.

The calibration was repeated recently with a 9-inch long flat reference, of which the flatness is also measured with the same FizCam 1500 without the null lens. To calibrate the null lens, the flat was mounted in front of the null lens, and was translated laterally to an azimuthal position for a measurement. The roll angle was precisely controlled by a hexapod to ensure normal incidence and proper retro-reflection into the interferometer. The angle was uniquely determined from the azimuthal position. Measurements were done at 2° steps, covering again about 56°. The resulting sag, as a function of azimuth, was derived and shown in Figure 1.

It can be seen that, overall, the null lens produces a rather large curved wavefront in the axial direction, about 3 μm over a 200 mm length, equivalent to having a radius of curvature of about 2 km at the distance of measurement. The wavefront is convex (sphere-like) in the axial direction.

It is seen that the average sag over the 56° range is 2.82 μm, and this has to be corrected for mirror metrology. Compared to previous calibration, the sag is slightly smaller: the average sag from previous calibration over the same range is 2.67 μm. This implies a difference of 0.15 μm overall, and more than 0.2 μm at particular azimuth, such as in the region around -8°. Part of the average difference may be attributed to the uncertainty in the determination of the physical length of the profile. Due to a lack of axial fiducials, the measured profile is assumed to have a full length of 217 mm. However, data dropouts due to insufficient reflection or poor performance at the axial ends of the null lens may produce a measured axial length shorter than 217 mm. An error of 2.5% in length is sufficient to explain the general difference of the sag over the full azimuthal range. This implies a loss of data from about 2.7 mm from each end of the null. Whether this was the case is not clear at this point of the study. At any rate, the difference implies that the absolute measurement of sag using this 60° null is not certain to better than about 0.1 – 0.2 μm, at least for comparison of measurements separated by a long time. Relative measurement, as shown below, is generally much more precise.

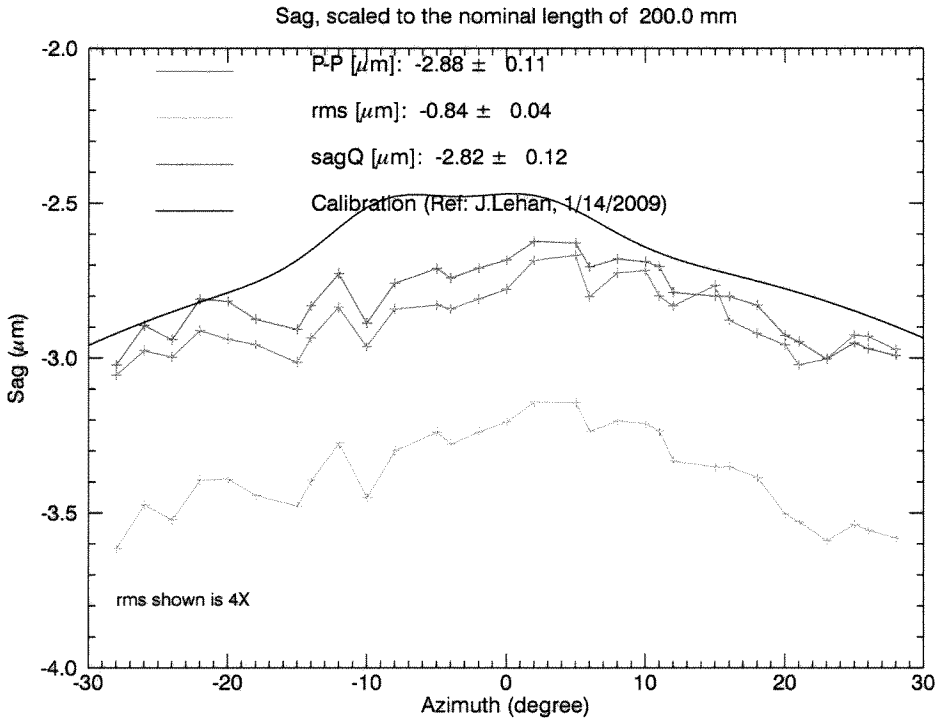

Figure 1. Dependence of axial sag from the FizCam 1500 system with the 4-element 60° null. The sag is normalized for the nominal length of 200 mm. Also shown are the peak-to-peak values of the axial profiles and their rms values (bottom curve, x4 for display purpose.) The smooth curve is the calibration done 2.5 years ago.

We also note the more marked mismatch in the -20 - 5° range. This seems to represent a genuine discrepancy. Also noted are the features at $\phi = -10°$ and $\phi = -15°$, where the sags seem to decrease abruptly by nearly 0.2 μm. It is not clear if there is such dip in the previous calibration, as much larger 5° increments were used.

For the FizCam 2000 with 36-degree Cylindrical Null, previous calibration established the sag at 0.3 μm, uniform across azimuth of the null lens.

2.2 Comparison of Calibrations with a cylindrical reference segment.

To examine the reliability of the measurements, especially of the sag, we compared measurements of the same cylindrical piece with the two instruments. Due to the aforementioned reflectivity limits of the two interferometers, a mirror with very high reflectivity cannot be measured with the same instrument. To enable cross-calibration with the same reference, we used a 'quasi-mirror' with no or just a thin coating as a reference. The reference is a relatively thick, 1.1 mm, substrate thermally slumped in a similar way as the ordinary 0.4 mm. Even though the thick substrate is not formed to high precision as it was harder to be slumped precisely and the process was not optimized for this thickness, the thermally formed piece did have a nice rough cylindrical form that was measurable. The thick mirror also provided a larger thermal mass and therefore improved thermal stability due to temperature fluctuations of the environment or from extraneous thermal source (mirror measurement is sensitive to thermal variation, see section 3.3.) It was also stiff and was more stable against variation in frictional forces from mounting. We use a kinematic method as the metrology mount (KB3) as it is demonstrated both from finite-element modeling and from experimentation that the mount has good repeatability.

The segment was measured with both instruments with their associated null lenses. The measurement was repeated with the segment lightly coated. The resulting sag as a function of azimuth is shown in Figure 2. In the derivation of sag, $S(\phi)$, we used the latest calibration for FizCam 1500, which is, on the average, 0.15 μm lower than the old calibration. We continued to use a constant 0.3 μm as the calibrated reference for FizCam 2000. From Figure 2, it can be seen that the measurements generally compare well. The differences are close to zero and are nearly independent of ϕ. The fact that there are still features with moderate spatial frequency, especially for the uncoated segment, may be due to the fact that the measurement of the uncoated mirror made with FizCam 1500 was not of very high quality, since the reflectivity is too low for that instrument. The data were rather noisy in that case.

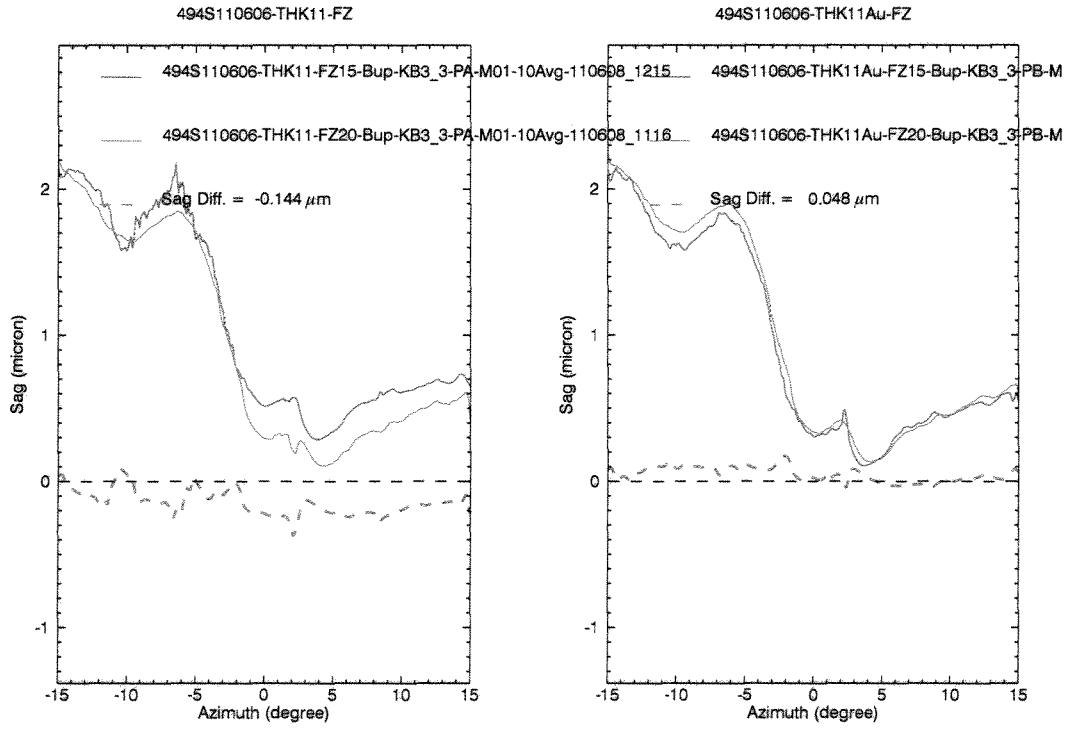

Figure 2. Comparisons of sag variation, for uncoated (left) and thinly coated (right) mirror. Comparison were between measurements made with FizCam 1500 + the 60° null and FizCam 2000 + 30° null . The differences in the two sag variations, shown as dashed curves, are close to zero and are nearly independent of azimuth. Especially for the coated mirror, the difference in calibration using the two systems is about 0.05 μm.

For the coated segment, the difference amount to 0.05 μm, on the average. This may be taken as the accuracy of the measured sag. The measurement of the uncoated segment compare less favorably. The comparison is less reliable, however. In addition to the noisy data mentioned above for FizCam 1500, there may be issues with extraneous fringes due to interference from the backside of the transparent glass. As pointed out earlier, this instrument, unlike the FizCam 2000, does not have a short coherence length, therefore it is not immune from backside reflection when the part is transparent.

As an aside, we note that comparison of the sag variations of the coated and uncoated segments, measured with the same instrument, indicates only 0.05 μm difference (with FizCam 2000, that with FizCam 1500 is also larger, but the same caveats mentioned above apply.) This serves as an indication of the limit of coating stress on sag. A more detailed study of coating stress is underway and will be reported elsewhere.

3. SURFACE MEASUREMENT REPEATABILITY

To properly gauge the reliability of the mirror surface metrology, we measured a specific mirror extensively under different measuring conditions. We would like to address the following specific questions: 1. How precise are the measurements themselves, once the mirror is placed in the metrology mount? 2. How does the metrology mount affect the measurement? How precise are the measurement if the mirror is removed from the mount and replaced? 3. How does the thermal condition affect the measurement? Again, since higher order axial parameters are usually preserved in such measurements, we will focus on the change in the low order axial errors, especially the sag.

3.1 Repeatability without mirror replacement

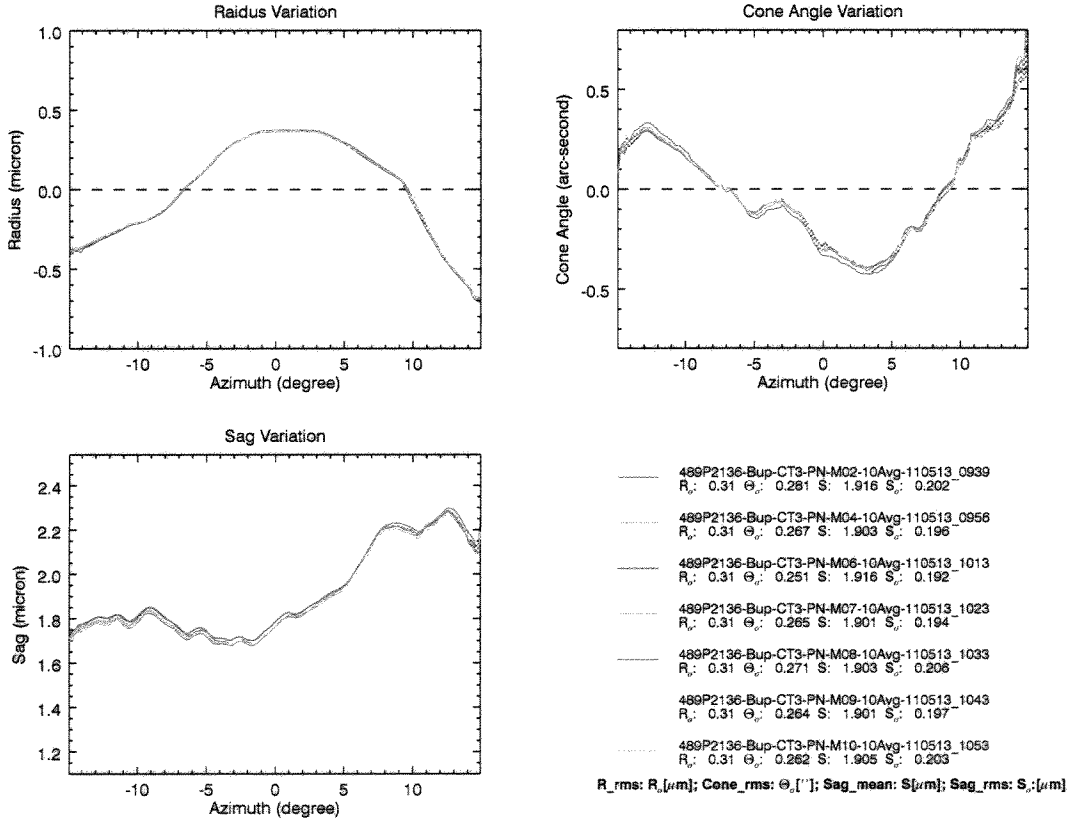

Figure 3. Axial Parameters from "measurement repeatability" of the mirror 489P2136, in the CT3 metrology mount. The measurements were repeated 7 times, without having the mirror replaced in the mount. There are 4 sets of such measurements. A summary is listed in Table 2.

To obtain a quantitative measure of the repeatability of the measurement, we first established the "measurement repeatability" by repeatedly measuring the same mirror (489P2136) without remounting it. This establishes the minimum repeatability due to various uncertainties of the measurement system and short-term stability of the environment.

Four sets of data were taken, two each of the "cantor-tree" mounts. These are vertical mounts in which the mirror was supported vertically by two rotatable slots at the bottom and constrained by 'clips' at the top. The numbers refer to the total number of points of constraints. CT3 has two mount points at the bottom and one clip at the top, whereas CT4 has two at the top. For each mount, the measurements were carried out in a single day and were repeated the next day. The mirror stayed in its mount in each set of measurement without being dismounted. A thermal box enclosed the mirror and the mount when these measurements were made. This is actually a subset of a larger set of data where the thermal box was sometimes removed and replaced, in order to establish the effect of thermal influence. The result detailing the thermal influences is discussed in the next section.

An example of the results is shown in Figure 3. From the analysis of these four sets of data, it is seen that the derived parameters are typically very consistent within each placement: Radius variation $\approx$ 0.1 μm, cone angle variation $\approx$ 0.1", sag $\approx$ 0.2 μm. The statistics of sag variation is summarized in Table 2.

Table 2 shows the sag of the mirrors from the 23 measurements. In the table, average sag is the mean of the sag across azimuth, and the sag variation is the rms value of the sag, as a function of azimuth, for each measurement. Overall, the sag variations agree quite well, to within $\approx$ 0.01 μm, from measurement to measurement within each set. Similar precision is obtained for the average sag. However, the sag variations and average sags are not consistent with these limits between the 4 sets of measurements, indicating larger "placement repeatability". The larger placement error is more outstanding for the data set CT3-"M". We will address this additional uncertainty in the next section.

Table 2. Summary of sag variations for the 4 sets of measurement repeatability.

Mount and Placement	Number of measurements	Average Sag (μm)	Sag Variation (μm)	ConeAngle Varation (arc-sec)
CT4 "M"	4	1.922 ± 0.007	0.158 ± 0.006	0.28 ± 0.03
CT4 "N"	5	1.912 ± 0.005	0.175 ± 0.013	0.17 ± 0.01
CT3 "M"	7	1.952 ± 0.014	0.245 ± 0.007	0.13 ± 0.01
CT3 "N"	7	1.906 ± 0.007	0.198 ± 0.005	0.27 ± 0.01

For the other parameters, such as the cone angle, similar dependence on alignment was also observed. Even though the cone angle is not an absolute measurement as mentioned above (there are certain components of the cone angle variation that are not measurable due to their elimination in the nulling of the fringes, and the absolute cone angle is not measured as there is no reference to absolute optical axis), the stability of the cone angle variation as a function of azimuth within each data set is evident from Table 2. Indeed, similar placement uncertainty occurred: The variations among the sets of data are significantly larger than that within the set ($\approx$ 0.01").

3.2 Placement repeatability and Mirror Mounting

To further study the effect of the placements of the mirror into the metrology mount, the same mirror was placed several times in the mount. In addition to the 4 sets of data shown in section 3.1 (CT3-M and -N, CT4-M and -N) we made specific measurements with repeated mounting and dismounting of the mirror using CT3. A total of 10 sets were taken and included in this analysis, even though, for four of these data sets, there was only one measurement. The new measurements were designated as placement "O" through "T". The remounting of mirror was also made at different times to simulate the actual measurement conditions. The results are summarized in Table 3.

Let's first consider the average sag. The average sag ranges from 1.88 μm to 2.02 μm, with a range of 0.14 μm and a standard deviation of 0.04 μm. The mean value of the average sag is 1.94 μm. There is apparently no significant difference of average sag between CT4 and CT3 mounts. The difference of mean values between CT3 and CT4 mounts from the mean value is 0.02 μm, which is statistically insignificant. The variance of average sag of measurements without replacement, ranging from 0.005 μm to 0.014 μm, however, is much smaller than that of the variation of the whole sample 0.04 μm. This is not unexpected as, from experience, we know that the average sag from typical

measurement is not as repeatable as 0.01 μm. The additional error from placement can come from variance in frictional force or change in environment, such as the thermal condition or possibly other mechanical drift in the alignment.

Table 3. Statistics of sag and cone angle variation of the 10 sets of mirror placement repeatability. In addition to the 4 sets of data used in Table 2, measurements "O" – "T" were made. Measurements O, P, Q and R were made once with remounting of the mirror. Measurements S and T were made with repeated taking of data after re-loading. It should also be noted that some of the measurements in the set of S and T were made on different days.

Mount and Placement	Number of measurements	Average Sag (μm)	Sag Variation (μm)	ConeAngle Varation (arc-sec)
CT4 "M"	4	1.922 ± 0.007	0.158 ± 0.006	0.28 ± 0.03
CT4 "N"	5	1.912 ± 0.005	0.175 ± 0.013	0.17 ± 0.01
CT3 "M"	7	1.952 ± 0.014	0.245 ± 0.007	0.13 ± 0.01
CT3 "N"	7	1.906 ± 0.007	0.198 ± 0.005	0.27 ± 0.01
CT3 "O"	1	2.02	0.28	0.16
CT3 "P"	1	1.92	0.21	0.17
CT3 "Q"	1	1.88	0.35	0.22
CT3 "R"	1	1.93	0.26	0.25
CT3 "S"	2	1.98 ± 0.07	0.26 ± 0.05	0.22 ± 0.1
CT3 "T"	6	1.95 ± 0.03	0.25 ± 0.02	0.18 ± 0.05

Nevertheless, we should note that, for the 2 measurements in placement `S', the difference is quite significant. In fact, the difference in average sag in that sample was 0.1 μm, which is an order of magnitude larger than the typical variation (rms) without mirror replacement. Therefore, if larger difference in the data set of placement "S" is not an anomaly due to the small sample (of size 2), it is an indication that the effect of placement of mirror may be smaller than the effect due to some (yet unknown) change in the environment. Similar difference can be seen for placement "T", between M-01 and the rest of the data sets (not shown in Table 3). Measurement 'PT-M01' was made on a different day than the rest of the sets. Could it be some residual thermal change, despite the enclosure of the mirror with a thermal box? Or could it be some other environmental change that cause a drift of the system (for example, the null lens may be cooler in the morning for quite a while, as it thermally lags behind the air and the mirror)? This is still to be explored.

For sag dependence on azimuth, the rms values are, curiously, typically larger for CT3 than CT4. The average of sag dependence (on azimuth) for the 2 CT4 placements is 0.17 μm, while that of 8 CT3 placements is 0.26 μm. The standard deviation of the CT3 samples is 0.05 μm. The difference is statistically quite significant. Similar conclusions can also be drawn from considering the sag variation and cone angle variation.

The cone angle variation on azimuth is, on the average, 0.20", with a standard deviation of 0.05". This variation is quite a bit larger than that without mirror replacement. The measurement repeatability without mirror replacement is typically 0.01", except for data set "T". This implies that, as for sag and sag variation on azimuth, the cone angle variation on azimuth also is significantly larger when the mirror was replaced. The set "T" should be considered special since additional variation was made in the measurement of "T", from measurements M04 through M06. For PT-M04, the mirror was moved towards the mirror T-side (a label we used to designate the right side of the mirror when viewing it with its larger end on top) by 10 mm; where for PT-M05, the mirror was moved towards the mirror E-side (the left side in the same viewing configuration) by 10 mm. The mirror was re-set to the 'nominal' middle for PT-M06. It was seen that (see also Figure 4) the cone angle was significantly different for M04 through M06, implying that shifting the mirror sideway may have consequence in cone angle variation but it does not affect sag variation. The cone angle variation can be affected due to a change in yaw from imperfect parallelism of the translational stage, for example. The sag, on the other hand, is not expected to sensitively depend on a small change in yaw.

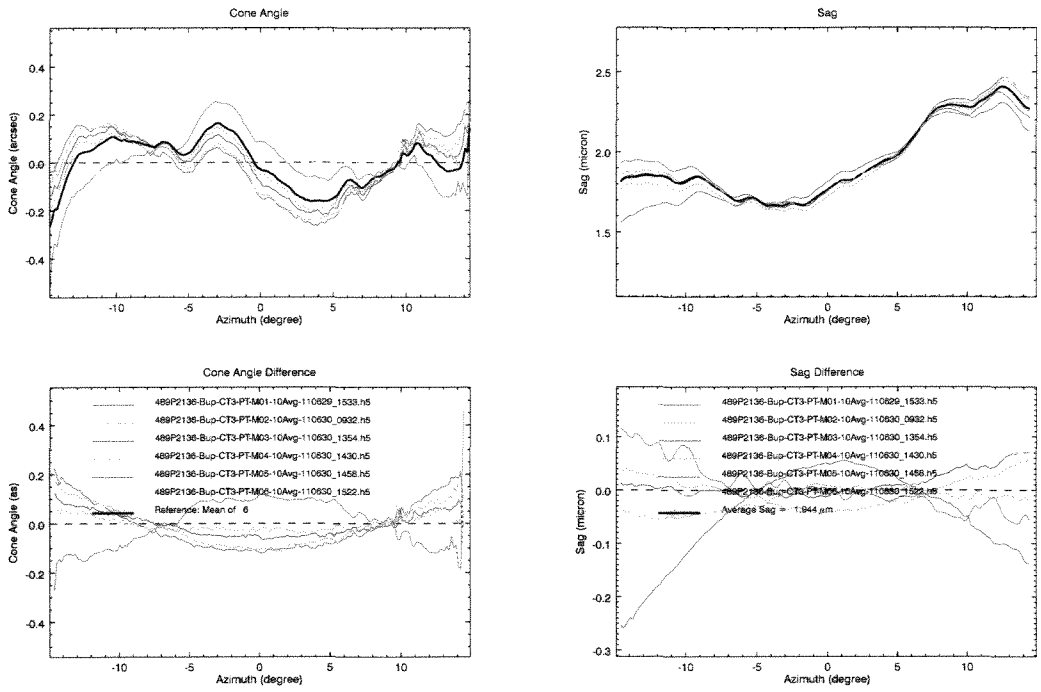

Figure 4. (Left) Cone angle variation on azimuth, for placement "T". Note that there are significant deviations from the mean due to deliberate misalignment of the mirror with respect to the null lens center meridian. The mirror was translated sideway starting from M04. (Right) Sag variation on azimuth for the same measurements of the "T" placement. Note that PT-M01 was measured on 6/29/2011 while the rest were measured on 6/30/2011.

3.3 Thermal effects

It was observed in the routine measurements of mirror that the measured parameters are sensitive to the environment. The variation of thermal environment can be attributed to a number of sources. The temperature of the laboratory in which the measurements were made was not actively controlled by the experimenters, but regulated by the building operation. The temperature changes, especially in very hot summer days and cold winter days, can be more than 1°C in the laboratory. The temperature cycle, naturally, is diurnal. Temperature variation was observed also at the location of the measurement, despite the fact that the whole set up, optical bench included, was enclosed in a plastic tent. In fact, with the enclosure, there is a vertical temperature gradient in the tent that is due to the heat released from the interferometer. This temperature gradient is more static or varying depending on how long the instrument is turned on.

Table 4. Summary of low order parameters measured for a mirror with or without the thermal enclosure. Four data sets were taken with two different metrology mounts.

	with thermal enclosure				without thermal enclosure			
Data Set	N	Av. Sag (μm)	Sag Var. (μm)	Cone Ang. Var. (arc-sec)	N	Av. Sag (μm)	Sag Var. (μm)	Cone Ang. Var. (arc-sec)
CT4 "M"	4	1.652 $\pm$0.007	0.132 $\pm$0.004	0.280 $\pm$0.034	7	1.715 $\pm$0.054	0.163 $\pm$0.021	0.308 $\pm$0.047
CT4 "N"	5	1.642 $\pm$0.005	0.142 $\pm$0.012	0.170 $\pm$0.011	7	1.721 $\pm$0.043	0.151 $\pm$0.016	0.194 $\pm$0.019
CT3 "M"	7	1.682 $\pm$0.014	0.208 $\pm$0.007	0.134 $\pm$0.009	3	1.719 $\pm$0.017	0.215 $\pm$0.018	0.134 $\pm$0.008
CT3 "N"	7	1.636 $\pm$0.007	0.163 $\pm$0.005	0.266 $\pm$0.009	3	1.675 $\pm$0.032	0.161 $\pm$0.013	0.275 $\pm$0.014

It was also found that the fluorescence lights in the laboratory cause significant temperature fluctuation. Monitoring of the temperatures showed that the temperature diurnal cycle was substantially smaller sub-°C during the weekend (when the lights are either on or off.) Direct experimentation of switching the lights on and off verify both the temperature fluctuation and measurement stability. We now leave the lights in the laboratory on all the time, in order to maintain as steady a room temperature as possible.

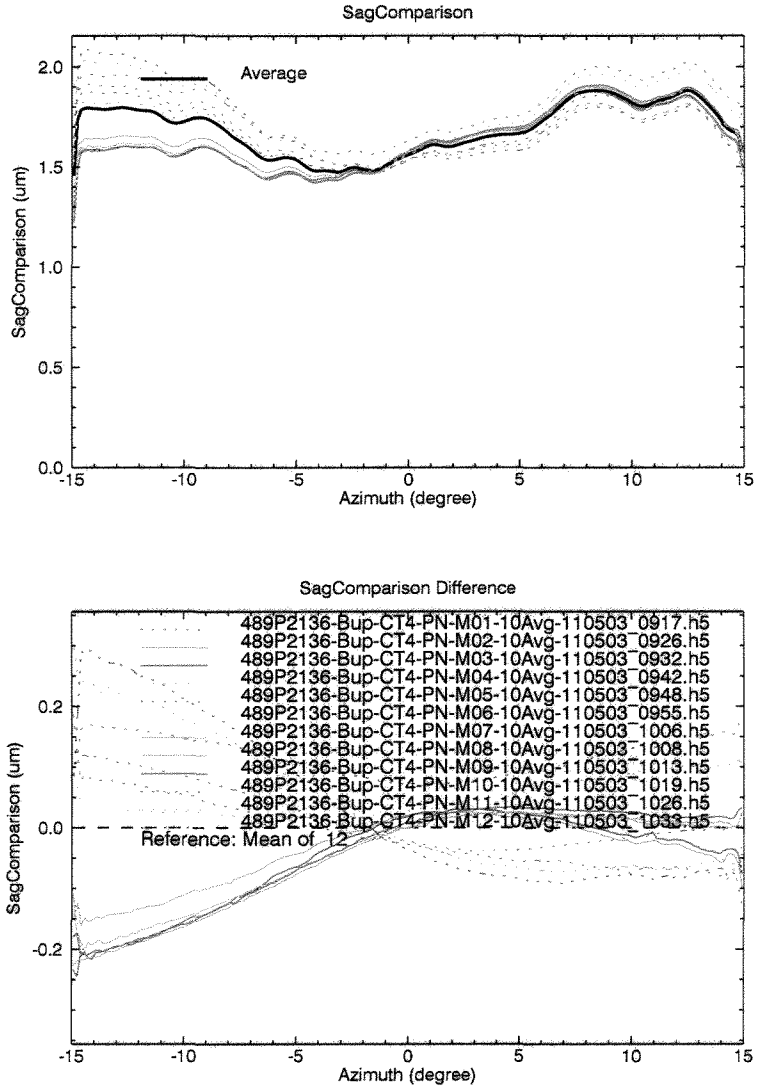

Figure 5. Sag variation of mirror in the metrology mount. Solid curves are for the measurements with the thermal box closed. Dashed curves are for the measurements in which the thermal box is either open or removed. Measurements were made with at least 15 minutes of wait time after the thermal box was removed or replaced. It is clear that the measurements are significantly more stable when the thermal box was in place and closed.

Another thermal source is the body heat from the operators. Infrared radiation from the operators directly affects the measurement. Direct experimentations with operators inside the tent demonstrated a dramatic asymmetric distortion of the mirror depending on the side the operator positioned. A strict code is now in place to make sure that the operator is outside the tent for some time when a measurement is to be made. The plastic shield of the tent is infra-red opaque.

With the basic understanding of the thermal effects on the measurements of mirrors, a series of tests were set up to explore the thermal sensitivity. In the test, a mirror is placed in a metrology cantor-tree mount (CT3 or CT4) and was

measured with the FizCam 2000 system with the 36° null. In the standard set up, the mirror is enclosed in a thermal box made of Styrofoam and lined inside with multi-layer insulating (MLI) material on 5 sides of the box. The bottom is the bare surface of the optical bench. A small window of the size of the null lens housing is necessarily open for the optical beam to come through for measurement. In some of the measurements, the thermal box is either removed or opened on one side.

Four sets of data were collected, each consisting of about a dozen measurements. Two sets were done with each of the CT3 and CT4 mounts. An example on the dependence of sag variation on the thermal setting is shown in Figure 5. Other data sets (all together 43 measurements were made) are similar. The data are summarized in Table 4.

It is clear, from Table 4 (and Figure 5), that there is substantially more variation in the parameters if the enclosure is removed. For instance, the average sag and sag variation for all the measurements, regardless of metrology mounts, were about 0.01 μm or less for the data taken with the thermal enclosure, while those taken without were several times larger, ranging from ≈ 0.02 – 0.05 μm. That effect for the cone angle variation is generally seen but the difference is not as large.

We have started to build up thermal models of the mirror segments. To complete the modeling, we need to obtain precise measurement of the temperature distribution and its variation of the mirrors as well as the exact nature of the constraint of the mirrors. Thermal models show that the figure of a bonded mirror depends very sensitively on the bulk temperature change. Under the current bonding configuration, the distortion can be as much as 20 arc-second (HPD) per °C of temperature difference between the mirror and its titanium housing. However, for a mirror in metrology mount (not constrained except by friction at a few points), the analysis is not as clear-cut. Some sort of temperature gradient may be needed to explain the distortion.

4. DISCUSSION

4.1 Summary of normal incidence metrology

In summary, we have established the optical normal incidence methods as a reliable metrology of thin, segmented x-ray mirrors. The use of Fizeau interferometers coupled with cylindrical null lenses, is capable of reliably characterizing thin mirror in scales from 200 mm down to sub-mm "mid-frequency" scale. The method is also very efficient. We have calibrated the null lenses to ≈ 0.1 μm accuracy in sag. The calibration was also confirmed by cross calibrating with a cylindrical segment. Further work is needed to calibrate the null and interferometer systems to < 0.1 μm. Absolute calibration of null orientation and position will be needed to derive the average radius or cone angle of the mirror segments. These are work in progress.

Stability of measurements was demonstrated to better than 0.01 μm when the segment is not dismounted from the metrology mount and remounted. The stability was significantly worse if the mirror is dismounted and reloaded, to ≈ 0.03 μm (rms) for mean sag or sag variation. Individual measurements, of course, can vary up to yet a few times larger in magnitude.

Thermal effect was demonstrated to affect measurements significantly. Diurnal temperature cycles in the laboratory add substantial uncertainty (as large as few times 0.1 μm of sag at particular azimuth) if the part is not thermally shielded. Subtle effects such as heat radiated from operators and lights in the laboratory are also significant. To minimize the impact from thermal variation, we have installed a thermal box to insulate these heat sources, in addition to containing the whole instrument and its optical bench in a plastic tent that is infra-red opaque. Further improvement in measurement stability from thermal disturbance will rely on thermal modeling and careful measurements of mirror temperature distribution.

4.2 Remarks on grazing incidence characterization

Besides the optical normal incidence characterization of the mirrors addressed in this paper, we have established grazing incidence methods to characterize the mirror. These methods complement the normal incidence optical measurements, especially in the area that the metrology described in the previous sections are either ineffective or imprecise. Even though we did not discuss these methods here, they are part of the overall effort in mirror characterization. These other metrologies are grazing incidence measurements that provide additional information such as the mean cone angle that determines the focal length of the mirror.

We currently employ two grazing incidence measurements to characterize mirrors. One is an optical Hartmann sub-aperture test which effectively measures the mean cone angle of the mirror. Additional information on low order figure of the mirror surface can be retrieved with wavefront sensing techniques[10]. We have set up a vertical alignment tower in which mirrors are placed in an optical beam. A Hartmann mask is used at the exit end of the mirrors for sub-aperturing. The mask is motorized and is controlled through computer software. Images captured on a large-format charge-coupled device is analyzed in real time to provide orientation parameters of the mirrors (which is used as a input for alignment iteration.) Measurement and analysis are automated so that measurements can be made without human intervention once the mirror, mask and camera are set up. Grazing incidence x-ray measurements are used as the final, definitive method of characterizing the x-ray mirrors, including its mounting, and its stability after bonding. Both the alignment and x-ray measurement were detailed in previous publications[11,12], and latest results will be published elsewhere.

REFERENCES

[1] Lehan, J. P., Atanossova, M., Chan, K.W., Hadjimichael, T., Saha, T.T., Hong, M., Zhang, W. and Blake, P., "Progress toward a complete metrology set for the International X-ray Observatory," Proc. SPIE, 7437, 74370R (2009).

[2] Lehan, J.P., Byron, G., McClelland, R., Hadjimichael, T., Russell, R., Robinson, D., "An alignment procedure for multi-element precision cylinder lenses and modular enclosure to house them," Proc. SPIE 7433, 7433-7 (2009).

[3] Civitani, M., Ghigo, M., Citterio, O., Spiga, D., Pareschi, G., Proserpio, L., "3D characterization of thin glass x-ray mirrors via optical profilometry," Proc. SPIE, 7803, 78030L (2010).

[4] Gubarev, M.V., O'Dell, S.L., Kester, T.J., Lehner, D.L., Jones, W.D., Smthers, M.E., Content, D.A., Reid, P.B., "Incoming metrology of segmented x-ray mandrels at MSFC," Proc. SPIE, 5494, 447 (2004).

[5] Content, D.A., Colella, D., Hadjimichael, T., Lehan, J.P., McMann, J., Reid, P.B., Saha, T., Zhang, W., "Optical metrology for the segmented optics on the Constellation-X Spectroscopy x-ray telescope," Proc. SPIE, 5488, 272 (2004).

[6] Jimenez-Garate, M.A., Craig, W.W., Hailey, C.J., Christensen, F.E., Jussain, A., "Fabrication, performance, and figure metrology of epoxy-replicated aluminum foils for hard x-ray focusing multilayer-coated segmented conical optics," Opt. Eng. 39(11), 2982 (2000).

[7] Freeman, M., Reid, P., Podgorski, W., Caldwell, D., "Advances in the Active Alignment System for the IXO optics," Proc. SPIE, 7732, 773243 (2010)

[8] Kuchel, M., "Interferometric measurement of rotationally symmetric aspheric surfaces," Proc. SPIE, 7389, 738916 (2009)

[9] Gao, G., Lehan, J.P., Zhang, W., Grlesmann, U., Soons, J.A., "Computer-generated hologram cavity interferometry test for large x-ray mirror mandrels: design," Opt. Eng., 48(6), 063602 (2009).

[10] Saha, T., Rohrbach, S., Hadjimichael, T., Zhang, W., "Wavefront sensing of X-ray Telescopes," Proc. SPIE, 7732, 77322S (2010)

[11] Chan, K.W., Zhang, W., Evans, T., McClelland, R., Hong, M., Mazzarella, J., Saha, T., Jalota, L., Olsen, L., Byron, G., "Mounting and Alignment of IXO Mirror Segments," Proc. SPIE, 7732, 77323Q (2010)

[12] Chan, K.W., Zhang, W., Saha, T., Robinson, D., Olsen, L., McClelland, R., Mazzarella, J., Lozipone, L., Lehan, J., Hong, M., Fleetwood, C., Evans, T., Byron, G., Larimore, J., "An Approach for Alignment, Mounting and Integration of IXO Mirror Segments," Proc. SPIE, 7437, 74371D (2009)